Graphene Nanoribbons Derived From Zigzag Edge-Encased Poly(*para*-2,9-dibenzo[*bc,kl*]coronenylene) Polymer Chains

Doreen Beyer,[†] Shiyong Wang,[‡,#] Carlo A. Pignedoli,[‡] Jason Melidonie,[†] Bingkai Yuan,[#] Can Li,[#] Jan Wilhelm,[¶,⊥] Pascal Ruffieux,[‡] Reinhard Berger,[†,*] Klaus Müllen,[§] Roman Fasel[‡,∥,*] and Xinliang Feng[†,*]

[†]Center for Advancing Electronics Dresden (cfaed) and Faculty of Chemistry and Food Chemistry, Chair for Molecular Functional Materials, Dresden University of Technology, 01062 Dresden, Germany

[‡]Empa, Swiss Federal Laboratories for Material Science and Technology, 8600 Dübendorf, Switzerland

[∥]Department of Chemistry and Biochemistry, University of Bern, Freiestrasse 3, 3012 Bern, Switzerland

[§]Max Planck Institute for Polymer Research, Ackermannweg 10, 55128 Mainz, Germany

[#]Department of Physics and Astronomy, Shanghai Jiao Tong University, 200240 Shanghai, China

[¶]Department of Chemistry, University of Zürich, 8057 Zürich, Switzerland

Supporting Information Placeholder

ABSTRACT: In this work, we demonstrate the bottom-up on-surface synthesis of poly(*para*-dibenzo[*bc,kl*]-coronenylene) (**PPDBC**), a zigzag edge-encased analog of poly(*para*-phenylene) (PPP), and its lateral fusion into zigzag edge-extended graphene nanoribbons (**zeeGNRs**). Towards this end, we designed a dihalogenated di(*meta*-xylyl)anthracene monomer displaying strategic methyl groups at the substituted phenyl ring and investigated its applicability as precursor in the thermally induced surface-assisted polymerization and cyclodehydrogenation. The structure of the resulting zigzag edge-rich (70 %) polymer **PPDBC** was unambiguously confirmed by scanning tunneling microscopy (STM) and non-contact atomic force microscopy (nc-AFM). Remarkably, by further thermal treatment at 450 °C two and three aligned **PPDBC** chains can be laterally fused into expanded **zeeGNRs**, with a ribbon width of nine ($N = 9$) up to seventeen ($N = 17$) carbon atoms. Moreover, the resulting **zeeGNRs** exhibit a high ratio of zigzag (67 %) vs. armchair (25 %) edge segments and feature electronic band gaps as low as 0.9 eV according to gaps quasiparticel calculations.

Bottom-up synthesized atomically precise graphene nanoribbons (GNRs) represent an imperative class of one-dimensional graphene nanostructures because of their outstanding electronic and magnetic properties, which entirely depend on their molecular topology at a width scale below 5 nm.[1–4] In comparison to other bottom-up protocols for GNR synthesis such as in solution[4,5] or by chemical vapor deposition (CVD)[6] under ambient pressure, the on-surface approach under ultrahigh vacuum conditions (UHV) has the advantage of giving access to characterization by *in-situ* scanning tunneling microscopy (STM), scanning tunneling spectroscopy (STS) and non-contact atomic force microscopy (AFM) to reveal the geometric and electronic structure of the prepared GNRs with atomic resolution.[2,7,8] Hitherto, a series of armchair,[2,7,8] chevron,[3,9,10] and few GNRs with other edge topographies - for example cove[11] and chiral[12–14] ones - have been fabricated via on-surface synthesis. In

2016, a fully zigzag edged GNR (ZGNR) has been successfully synthesized on an Au(111) substrate using an "U-shaped" monomer.[15] The key strategy employed is to take advantage of a methyl group substituted umbrella-shaped precursor monomer forming a snake-like polymer chain in a thermal annealing step. Subsequent methyl group activation provides the missing carbon atoms to build up the zigzag edge periphery.[15] In contrast to the rich portfolio of accessible monomer designs for the on-surface synthesis of armchair edged GNRs (AGNRs), so far this is the only design principle available for an entirely zigzag edged GNR.

Herein, we report the surface-assisted bottom-up synthesis of a partial zigzag edge terminated poly(*para*-dibenzo[*bc,kl*]coronenylene) polymer (**PPDBC**, Fig. 1c) - a strictly linear zigzag edge extended derivative of poly(*para*-phenylene) PPP - by polymerisation and subsequent cyclodehydrogenation of 9,10-bis(4-bromo-2,6-dimethylphenyl)anthracene (monomer **1**, Fig. 1a). Remarkably, the resulting **PPDBC** chains can undergo a "zipper process" (cross-dehydrogenation) leading to GNRs (**zeeGNRs**, Fig. 1d) with an extended alternating zigzag-armchair-periphery in a 6:1 ratio. Therefore, the strategy of **PPDBC** interchain fusion could be utilized to synthesize laterally zigzag edge-expanded GNRs (**zeeGNR1**, **zeeGNR2**) with variable ribbon widths comprising zigzag-rich edge topologies, which lead to low electronic band gaps, e.g. 0.9 eV for **zeeGNR2**. Interestingly, the resultant **zeeGNR1** and **zeeGNR2** can be identified as 8-AGNR-S(1,1.5) and 13-AGNR-I(1,3) respectively, according to the nomenclature of topological GNRs.[16,17]
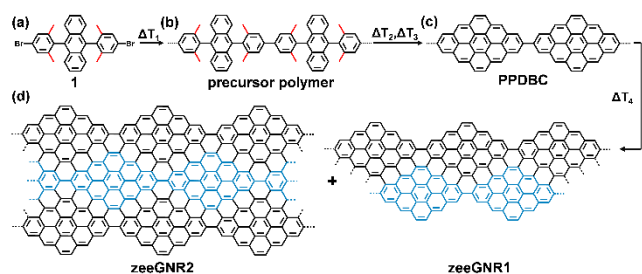
Figure 1. Bottom-up on-surface synthesis of zigzag edge-enriched graphene nanoribbons. Surface-assisted carbon-carbon coupling of (a) 9,10-bis(4-bromo-2,6-dimethylphenyl)anthracene (monomer **1**) on Au(111) under UHV conditions at 200 °C yields a (b) 1D precursor polymer. (c) Subsequent cyclodehydrogenation ($\Delta T_3 = 350$ °C) provides sp^2-hybrizied, aligned **PPDBC** chains. (d) A further thermal annealing step ($\Delta T_4 = 450$ °C) enables an intermolecular "zipping process" forming **zeeGNR1** and **zeeGNR2** on the surface.

As illustrated in Figure 1a we firstly designed and synthesized the dihalogenated di(*meta*-xylyl)anthracene molecular building block **1** comprising two methyl groups at each outer substituted phenyl ring to reach a novel type of rhombic-shaped polymer chain (**PPDBC**) (Fig. 1c) by on-surface Ullmann-type polymerization and cyclodehydrogenation driven by strategic methyl group activation at elevated temperatures. Specifically, the synthesis of monomer **1** (Fig. 2a) commenced with the nucleophilic addition of 5-bromo-2-iodo-1,3-dimethylbenzene to 9,10-anthraquinone providing 9,10-bis(4-bromo-2,6-dimethylphenyl)-9,10-dihydroanthracene-9,10-diol **2** as intermediate compound, which has been used without further purification. Afterwards the crude mixture was treated with glacial acetic acid, sodium iodide and sodium hypophosphite monohydrate for 1.5 h under reflux to afford the desired monomer **1** (9,10-bis(4-bromo-2,6-dimethylphenyl)anthracene) in 38 % yield over both reaction steps. The chemical identity of monomer **1** was unambiguously confirmed by two-dimensional nuclear magnetic resonance spectroscopy (NMR) (see Supporting Information) and high-resolution matrix-assisted laser desorption/ionization (HR-MALDI-TOF) as shown in Figure 2b.
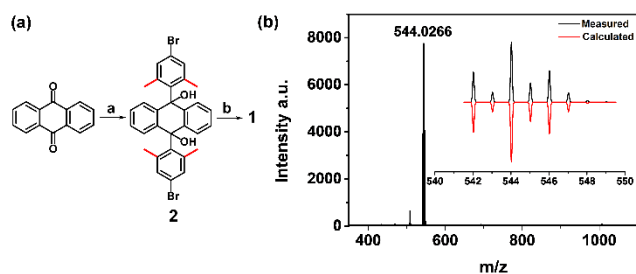
Figure 2. Synthesis and characterization of monomer 1. (a) Chemical reagents and conditions: (a) 5-bromo-2-iodo-1,3-dimethylbenzene, *n*-BuLi, THF, -78 °C, overnight, (b) sodium iodide, sodium hypophosphite monohydrate, glacial acetic acid, 135 °C, 1.5 h. (b) Liquid-state high-resolution MALDI-TOF spectra.

Thereafter, monomer **1** was deposited on a Au(111) single-crystal surface under UHV conditions and thermally annealed to induce and investigate the polymerization process. Self-assembled molecular islands of monomer **1** are detectable at room temperature (Fig. 3a-b). Within such islands, individual molecules are close-packed, with the assembly being stabilized by weak interactions (see Supporting Information). On-surface thermal annealing to

$\Delta T_1 = 200$ °C induces debromination and aryl-aryl coupling reaction via activated surface-stabilized radicals producing 1D covalently bonded polymer chains (Fig. 3c). Initiated by a second thermal annealing step ($\Delta T_2 = 250$ °C) the precursor polymers with an average chain length of 50 nm undergo already partial cyclodehydrogenation of the incorporated methyl groups, which leads to some isolated polymers with partially cyclodehydrogenated segments as highlighted by the white circle in Fig. 3d. By treatment at $\Delta T_3 = 350$ °C the construction of fully planarized, highly uniform **PPDBC** chains, featuring an overall zigzag edge percentage of 70 % (detailed explanation for the assignment of edges, see Supporting Information), is completed (Fig. 3e-f). High resolution non-contact atomic force microscopy (nc-AFM) was employed to elucidate the molecular structure of **PPDBC** using a CO-functionalized tungsten tip attached to a quartz tuning fork.[18] Figure 3e shows the nc-AFM image of a **PPDBC** chain segment using the previously described technique in a constant-height mode. The image clearly resolves the structure of a **PPDBC** segment with a length of ~10 nm that exhibits no defects at the chemical bond level, proving that the methyl group-based cyclodehydrogenation worked convincingly in a fully selective way. Due to the long-range alignment of the aromatic **PPDBC** wires (Fig. 3f) and their characteristic reactive zigzag periphery a lateral edge fusion, the so called "zipper process", gives rise to atomically precise **zeeGNRs** with zigzag edge-enriched geometry. Thermal annealing sets in the "zipper process" (see Supporting Information) and at elevated temperatures of $\Delta T_4 = 450$ °C a significant amount of fused **zeeGNRs** is formed (Fig. 3g). The resulting zigzag edge proportion of **zeeGNR1**, consisting of two laterally fused **PPDBC** chains (Fig. 3h), can be calculated to be 67 %. The percentage of zigzag periphery remains constant for further polymer chain fusions (see Supporting Information), e.g. **zeeGNR2** involving three **PPDBC** chains. In STM images (Fig. 3f-h), the rhombic-shaped **PPDBC** chains and the **zeeGNR1-2** exhibit equal apparent heights of ~ 170 pm.
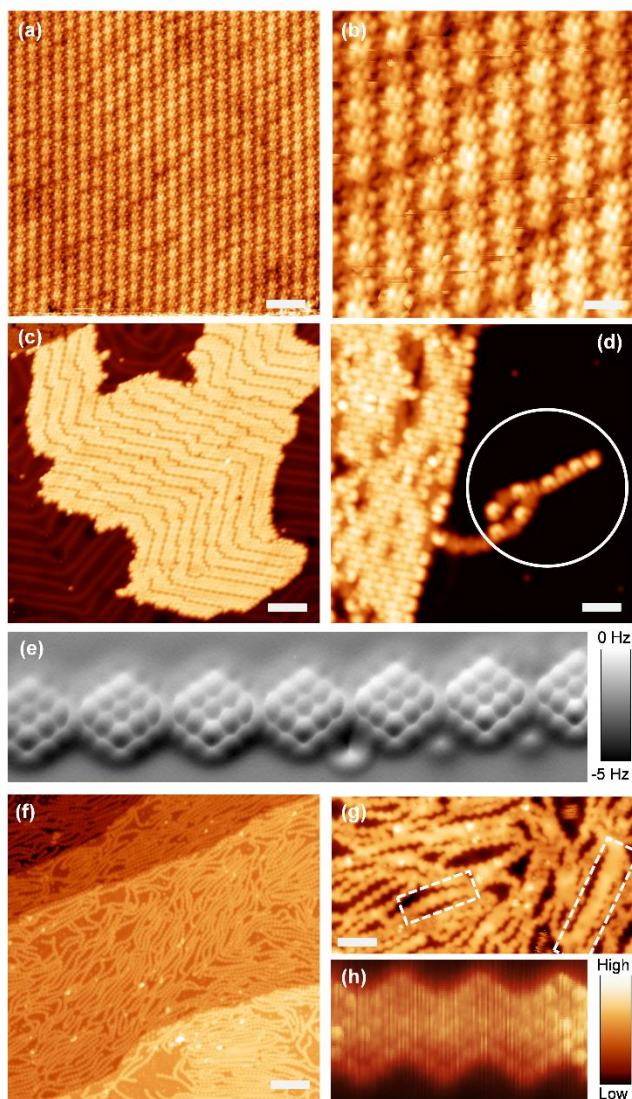
Figure 3. nc-AFM and STM imaging of the bottom-up synthesis of highly aligned PPDBC chains and zeeGNRs. STM images of (a-b) a molecular island of monomer **1** after room temperature deposition. Scale bar: 5 nm, I = 50 pA, V = -0.1 V. Thermal annealing at $\Delta T_1 = 200$ °C generates (c) covalently bonded polymer chains. Scale bar: 5 nm, I = 20 pA, V = -0.6 V. Further thermal treatment at $\Delta T_2 = 250$ °C induces (d) partial cyclodehydrogenation. Scale bar: 5 nm, I = 20 pA, V = -0.6 V. (e) Constant-height nc-AFM frequency shift image of a uniform **PPDBC** segment using a CO-functionalized tip, after rising the temperature to $\Delta T_3 = 350$ °C. $A_{osc} = 70$ pm, V = 5 mV. Large-scale STM image of (f) **PPDBC** chains. Scale bar: 5 nm, I = 30 pA, V = - 0.6 V. (g) Further thermal annealing at $\Delta T_3 = 450$ °C produces zigzag edge-extended graphene nanoribbons (**zeeGNRs**) with diverse ribbon width and mixed zigzag-armchair periphery. The dashed white rectangles highlight zipped zeeGNRs (**zeeGNR1**, **zeeGNR2**) with double and triple width of **PPDBC**, respectively. Scale bar: 5 nm, I = 30 pA, V = 0.6 V. (h) Constant-height current image of a **zeeGNR1** fragment using a CO functionalized tip. V = 1 mV.

The electronic band structures of **PPDBC**, **zeeGNR1** and **zeeGNR2** were computed by density functional theory (DFT) (Fig. 4d). DFT revealed a non-magnetic ground state for the **PPDBC** system in gas phase and an electronic energy gap of $\Delta = 1.1$ eV

(Fig. 4d). For higher-order structures (nanoribbons) achieved through interchain fusion of **PPDBC** the band gap decreases with increasing ribbon width to $\Delta = 0.85$ eV (**zeeGNR1**) and $\Delta = 0.15$ eV (**zeeGNR2**), respectively (Fig. 4d). Scanning tunneling spectroscopy (STS) was employed to obtain experimental band gap data for the surface confined polymer/ribbon systems. As shown in Figure 4c, differential conductance (dI/dV) spectra of **PPDBC** and **zeeGNR1** suggest a band gap of 1.7 eV and 1.4 eV, respectively. Differential conductance dI/dV mapping reveals the local density of states spatial distribution near the top of valence band and the bottom of conduction band (cf. Figure 4a-b). In dI/dV mapping we determined slightly higher energies for **PPDBC** and **zeeGNR1**, due to the stronger dI/dV signals. The band gap of **zeeGNR2** cannot be clearly resolved by STS measurements, mostly because of the energetic overlap of Au(111) surface states with nanoribbon frontier states. We notice that the measured energy gaps for **PPDBC** and **zeeGNR1** are much larger than the DFT calculated values. Not only does the Kohn-Sham gap significantly underestimate the band gap of bulk semiconductors[19], the discrepancy is amplified in low-dimensional materials, such as the quasi-one-dimensional GNRs or carbon nanotubes, where screening of the Coulomb interaction between electrons is strongly reduced.[20] Thereby, to obtain an accurate estimation of the band gaps, we performed quasiparticle GW[21] calculations in gas phase (see Supporting Information), obtaining values of 3.0 eV, 2.0 eV and 0.9 eV for **PPDBC**, **zeeGNR1** and **zeeGNR2**, respectively. A reduction of the band gap from the gas phase GW values of 3.0 eV for **PPDBC** and 2.0 eV for **zeeGNR1** to the values determined on Au(111) of 1.7 eV and 1.4 eV is in line with the expectations due to image charge effects.[22] In comparison to reported 5-($\Delta = 0.1$ eV),[8] 7-($\Delta = 2.4$ eV),[2] 9-($\Delta = 1.4$ eV)[23], 13-($\Delta = 1.4$ eV)[7] AGNRs and the fully zigzag edged 6-ZGNR ($\Delta = 1.9$ eV)[15], zigzag edge-enriched GNRs also host a highly tunable band gap, indicating their significance as precious member of the growing family of graphene nanostructures.
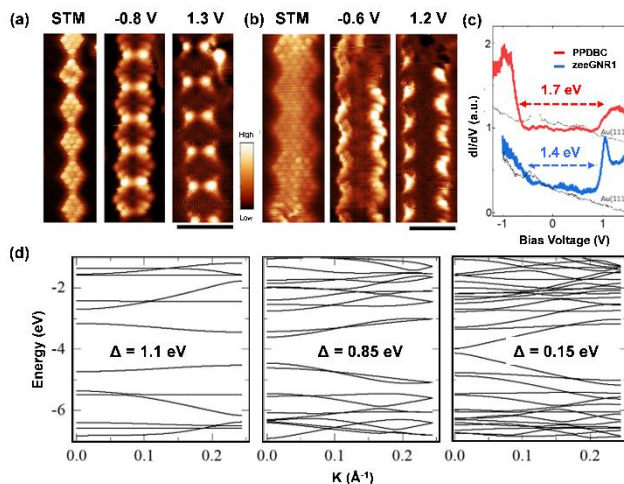
Figure 4. Band structure calculations and scanning tunneling spectroscopy. (a-b) Constant-height current image (V=1 mV), constant-current dI/dV mapping at the onset of valence band, and dI/dV mapping at the onset of conduction band for **PPDBC** and **zeeGNR1**, respectively. Scale bars: 2 nm. (c) dI/dV spectra taken at the edge of **PPDBC** and **zeeGNR1**, revealing an energy gap of 1.7 eV and 1.4 eV, respectively. The dashed black curves are spectra taken at the nearby clean Au(111) surface. (d) DFT calculated band structure of **PPDBC**, **zeeGNR1**, and **zeeGNR2**, respectively.

In summary, we demonstrated the on-surface synthesis towards high quality poly(*para*-dibenzo[*bc,kl*]coronenylene) polymer

chains, derived from a simple molecular polyphenylene precursor. The fully conjugated, aligned **PPDBC** polymers with predominant zigzag periphery and their exotic interchain-interaction paved the way for the successful zeeGNR fabrication with a zigzag edge content of 67 %, variable ribbon width, tunable electronic band structures and the possibility of synthesizing topological GNRs.[16,17] Prospectively, the combination of versatile substituted anthracene-like building blocks and the powerful on-surface chemistry approach enables to develop other multi-edged graphene nanostructures in order to study their crucial physical properties such as band structure and magnetism.

ASSOCIATED CONTENT

Supporting Information

The Supporting Information is available free of charge on the ACS Publications website at DIO:
Experimental section of monomer building block **1**, characterization by liquid-state NMR (^{1}H-, ^{13}C-, 2D-NMR) and high-resolution mass spectra (HR-MALDI-TOF, HR-ESI-MS) Furthermore details of on-surface sample preparation, STM and non-contact AFM measurements as well as DFT and GW calculations (PDF).

AUTHOR INFORMATION

Corresponding Author

*E-mail: reinhard.berger@tu-dresden.de
*E-mail: xinliang.feng@tu-dresden.de
*E-mail: roman.fasel@empa.ch

ORCID

Doreen Beyer: 0000-0002-7835-7857
Shiyong Wang: 0000-0001-6603-9926
Carlo A. Pignedoli: 0000-0002-8273-6390
Jason Melidonie: 0000-0003-0201-2075
Jan Wilhelm: 0000-0001-8678-8246
Pascal Ruffieux: 0000-0001-5729-5354
Reinhard Berger: 0000-0002-8959-7821
Klaus Müllen: 0000-0001-6630-8786
Roman Fasel: 0000-0002-1553-6487
Xinliang Feng: 0000-0003-3885-2703

Present Addresses

$^\perp$BASF SE, 67065 Ludwigshafen am Rhein, Germany

Author Contributions

Doreen Beyer and Shiyong Wang contributed equally to this work.

Notes

The authors declare no competing financial interests.

REFERENCES

(1) Cai, J.; Pignedoli, C. A.; Talirz, L.; Ruffieux, P.; Söde, H.; Liang, L.; Meunier, V.; Berger, R.; Li, R.; Feng, X.; Müllen, K.; Fasel, R. *Graphene Nanoribbon Heterojuction, Nat. Nanotechnol.* **2014**, *9* (11), 896–900.

(2) Cai, J.; Ruffieux, P.; Jaafar, R.; Bieri, M.; Braun, T.; Blankenburg, S.; Muoth, M.; Seitsonen, A. P.; Saleh, M.; Feng, X.; Müllen, K.; Fasel, R. A*tomically Precise Bottom-up Fabrication of Graphene Nanoribbons, Nature* **2010**, *466* (7305), 470–473.

(3) Celis, A.; Nair, M. N.; Taleb-Ibrahimi, A.; Conrad, E. H.; Berger, C.; de Heer, W. A.; Tejeda, A. *Graphene Nanoribbons: Fabrication, Properties and Devices, J. Phys. D. Appl. Phys.* **2016**, *49* (14), 143001.

(4) Dössel, L.; Gherghel, L.; Feng, X.; Müllen, K. *Graphene Nanoribbon by Chemists: Nanometer-sized, solubale and Defect-free, Angew. Chem. Int. Ed.* **2011**, *50* (11), 2540–2543.

(5) Narita, A.; Feng, X.; Hernandez, Y.; Jensen, S. a; Bonn, M.; Yang, H.; Verzhbitskiy, I. a; Casiraghi, C.; Hansen, M. R.; Koch, A. H. R.; Fytas, G.; Ivasenko, O.; Li, B.; Mali, K. S.; Balandina, T.; Mahesh, S.; De Feyter, S.; Müllen, K. *Synthesis of Structurally Well-defined and Liquid Phase-processable Graphene Nanoribbons, Nat. Chem.* **2014**, *6* (2), 126–132.

(6) Chen, Z.; Zhang, W.; Palma, C.-A.; Lodi Rizzini, A.; Liu, B.; Abbas, A.; Richter, N.; Martini, L.; Wang, X.-Y.; Cavani, N.; Lu, H.; Mishra, N.; Coletti, C.; Berger, R.; Klappenberger, F.; Kläui, M.; Candini, A.; Affronte, M.; Zhou, C.; De Renzi, V.; del Pennino, U.; Barth, J. V.; Räder, H. J.; Narita, A.; Feng, X.; Müllen, K. *Synthesis of Graphene Nanoribbons by Ambient-Pressure Chemical Vapor Deposition and Device Fabrication, J. Am. Chem. Soc.* **2016**, *138* (47), 15488–15496.

(7) Chen, Y. C.; De Oteyza, D. G.; Pedramrazi, Z.; Chen, C.; Fischer, F. R.; Crommie, M. F. *Tuning the Band Gap of Graphene Nanoribbons Synthesized from Molecular Precursors, ACS Nano* **2013**, *7* (7), 6123–6128.

(8) Kimouche, A.; Ervasti, M. M.; Drost, R.; Halonen, S.; Harju, A.; Joensuu, P. M.; Sainio, J.; Liljeroth, P. *Ultra-narrow Metallic Armchair Graphene Nanoribbons, Nat. Commun.* **2015**, *6*, 10177.

(9) Teeter, J. D.; Costa, P. S.; Mehdi Pour, M.; Miller, D. P.; Zurek, E.; Enders, A.; Sinitskii, A. *Epitaxial Growth of Aligned Atomically Precise Chevron Graphene Nanoribbons on Cu(111), Chem. Commun.* **2017**, *53* (60), 8463–8466.

(10) Vo, T. H.; Shekhirev, M.; Kunkel, D. A.; Orange, F.; Guinel, M. J.-F.; Enders, A.; Sinitskii, A. A. *Bottom-up Solution Synthesis of Narrow Nitrogen-doped Graphene Nanoribbons, Chem. Commun.* **2014**, *50* (32), 4172–4174.

(11) Liu, J.; Li, B.-W.; Tan, Y.; Giannakopoulos, A.; Sanchez-Sanchez, C.; Beljonne, D.; Ruffieux, P.; Fasel, R.; Feng, X.; Müllen, K. *Toward Cove-Edge Low Band Gap Graphene Nanoribbons, J. Am. Chem. Soc.* **2015**, *137* (18), 6097–6103.

(12) Sánchez-Sánchez, C.; Dienel, T.; Deniz, O.; Ruffieux, P.; Berger, R.; Feng, X.; Müllen, K.; Fasel, R. *Purly Armchair or Partially Chiral: Non-contact Atomic Force Microscopy Characterization of Dibromo-Bianthryl-based Graphene Nanoribbons Grown on Cu(111), ACS Nano* **2016**, *10* (8), 8006–8011.

(13) Wang, X. Y.; Urgel, J. I.; Barin, G. B.; Eimre, K.; Di Giovannantonio, M.; Milani, A.; Tommasini, M.; Pignedoli, C. A.; Ruffieux, P.; Feng, X.; Fasel, R.; Müllen, K.; Narita, A. *Bottom-up Synthesis of Heteroatom-Doped Chiral Graphene Nanoribbons, J. Am. Chem. Soc.* **2018**, *140* (29), 9104–9107.

(14) De Oteyza, D. G.; García-Lekue, A.; Vilas-Varela, M.; Merino-Díez, N.; Carbonell-Sanromà, E.; Corso, M.; Vasseur, G.; Rogero, C.; Guitián, E.; Pascual, J. I.; Ortega, J. E.; Wakayama, Y.; Peña, D. *Substrate-Independent Growth of Atomically Precise Chiral Graphene Nanoribbons, ACS Nano* **2016**, *10* (9), 9000–

9008.

(15)   Ruffieux, P.; Wang, S.; Yang, B.; Sanchez, C.; Liu, J.; Dienel, T.; Talirz, L.; Shinde, P.; Pignedoli, C. A.; Passerone, D.; Dumslaff, T.; Feng, X.; Muellen, K.; Fasel, R. *On-surface synthesis of graphene nanoribbons with zigzag edge topology*, *Nature* **2016**, *531* (7595), 489–493.

(16)   Gröning, O.; Wang, S.; Yao, X.; Pignedoli, C. A.; Borin Barin, G.; Daniels, C.; Cupo, A.; Meunier, V.; Feng, X.; Narita, A.; Müllen, K.; Ruffieux, P.; Fasel, R. *Engineering of robust topological quantum phases in graphene nanoribbons, Nature* **2018**, *560* (7717), 209–213.

(17)   Rizzo, D. J.; Veber, G.; Cao, T.; Bronner, C.; Chen, T.; Zhao, F.; Rodriguez, H.; Louie, S. G.; Crommie, M. F.; Fischer, F. R. *Topological band engineering of graphene nanoribbons, Nature* **2018**, *560* (7717), 204–208.

(18)   Gross, L.; Wang, Z. L.; Ugarte, D.; Mohn, F.; Moll, N.; Heer, W. a; Vincent, P.; Liljeroth, P.; Journet, C.; Meyer, G.; Binh, V. T.; Poot, M.; Zant, H. S. J. Van Der; Aguasca, A.; Bachtold, A.; Kim, K.; Zettl, A.; Hung, P.; Postma, H. W. C.; Bockrath, M.; Blase, X.; Roche, S. T*he Chemical Structure of a Molecule Resolved by Atomic Force Microscopy, Science* **2009**, *325*, 1110–1114.

(19)   Steven G. Louie; Cohen, M. L. *Conceptual Foundations of Materials A Standard Model for Ground- and Excited-State Properties*; 2006.

(20)   Yang, L.; Park, C. H.; Son, Y. W.; Cohen, M. L.; Louie, S. G. *Quasiparticle Energies and Band Gaps in Graphene Nanoribbon Phys. Rev. Lett.* **2007**, *99* (18), 6–9.

(21)   Hutter, J.; Iannuzzi, M.; Schiffmann, F.; VandeVondele, J. *cp2k: Atomistic Simulations of Condensed Matter Systems, Wiley Interdiscip. Rev. Comput. Mol. Sci.* **2014**, *4*, 15–25.

(22)   Blankenburg, S.; Cai, J.; Ruffieux, P.; Jaafar, R.; Passerone, D.; Feng, X.; Müllen, K.; Fasel, R.; Pignedoli, C. A. *Intraribbon Heterojunction Formation in Ultra-narrow Graphene Nanoribbons, ACS Nano* **2012**, *6* (3), 2020–2025.

(23)   Talirz, L.; Söde, H.; Dumslaff, T.; Wang, S.; Sanchez-Valencia, J. R.; Liu, J.; Shinde, P.; Pignedoli, C. A.; Liang, L.; Meunier, V.; Plumb, N. C.; Shi, M.; Feng, X.; Narita, A.; Müllen, K.; Fasel, R.; Ruffieux, P. *On-Surface Syntehsis and Characterization of 9-Atom Wide Armchair Graphene Nanoribbons, ACS Nano* **2017**, *11* (2), 1380–1388.